Numerical Simulation of Concentration Polarization to Estimate Gypsum and Calcium Carbonate Scaling on Membrane Surfaces

Asunción Santafé-Moros[1]*, José M. Gozálvez-Zafrilla[1]
[1]Institute for Industrial, Radiophysical and Environmental Safety (ISIRYM), Universitat Politècnica de Valencia
* Chemical and Nuclear Eng. Department. Universitat Politècnica de Valencia, C/ Camino de Vera s/n, 46022 Valencia, Spain, assanmo@iqn.upv.es

Abstract: In this work, a numerical model was developed to estimate the scaling parameters on a reverse osmosis membrane process. The model takes into account the concentration polarization of ionic species in the membrane channel of spiral-wound modules and the effect of the membrane spacers on the flow. As an example of application, the scaling potential of calcium carbonate and sulfate carbonate (gypsum) salts were studied, as they are common sparingly salts causing precipitates in desalination plants. The results showed cases where localized membrane scaling occurs in spite of not having scaling conditions in the bulk solution. Besides, a parametric study was performed to show the effects of the cross-flow velocity on the scaling potential. The developed model can be useful to determine suitable operating conditions to minimize the risk of scaling.

Keywords: membrane scaling, polarization, fouling, salt precipitation.

1. Introduction

One of the main concerns of membrane plant operators is to avoid salt precipitation on the membrane surface (scaling), which is produced when the salt solubility product is exceeded. Calcium sulfate (gypsum) and calcium carbonate are the most common salts forming precipitates in membrane desalination plants. The Langelier Saturation Index (LSI) for calcium carbonate, and the percentage of saturation for gypsum are the parameters most commonly used to evaluate the scaling potential of these salts.

In a desalination plant, several membrane modules are connected in series inside a pressure vessel (Fig. 1). Along the separation process, there is a gradual build-up of the ionic concentration as a consequence of the generation of a diluted permeate stream and the ionic rejection. Therefore, the scaling potential is higher in the last element of the system, as a consequence of its higher concentration.

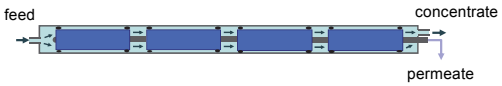

Figure 1. Pressure vessel containing modules in-series.

The standard procedure of scaling calculation starts estimating the concentrate composition from the feed composition for the system recovery required. Usually, the scaling parameters are calculated from the concentrate bulk composition. However, the concentration on the membrane surface can be significantly higher than that in the bulk solution due to the effect of concentration polarization. The concentration polarization is the increase of concentration in the boundary layer as a consequence of the rejection by the membrane of the ions transported by convective flow towards the membrane (Fig. 2). Therefore, the higher concentration in the membrane wall compared to that of the bulk implies a risk of scaling underestimation if the calculation are based on bulk conditions.

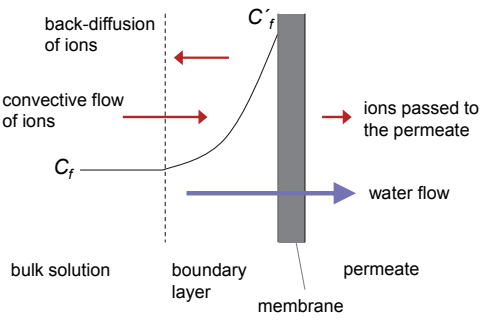

Figure 2. Concentration polarization near the membrane interface

The effect of concentration polarization can be minimized by incorporating spacers in the membrane channel as turbulence promoters [1]. CFD simulations can be used to assess their effect [2].

2. Domain of study

As mentioned before, the module under the worst scaling conditions is the one placed in the last position of the pressure vessel. Fig. 2 shows the internal structure of a spiral-wound membrane module (half of the module is unwound). A feed channel spacer is placed between two membrane leaves to create a channel for the stream that flows from feed to concentrate (in the direction indicated by the big arrow of the figure). The permeate flow that has passed through the membrane leaves is collected towards the permeate tube collector (in the direction of the small arrows).

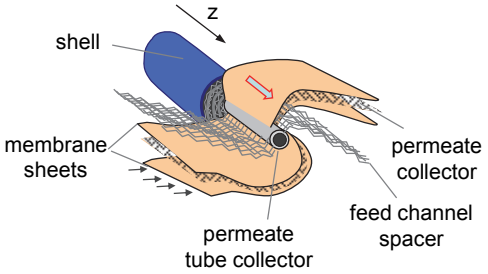

Figure 2. Spiral-wound module structure.

Fig. 3 shows the simplification procedure of the domain of study. For the last module (Fig. 3a), the variation of flow inside the channel is low, so, an arbitrary cylindrical element can be selected (Fig. 3b). In this cylindrical element, the flow conditions are independent of the φ-coordinate and little dependent on the r-coordinate. Therefore, a cross section can be taken as representative (Fig. 3c). Then, the domain selected for this study was a two-dimensional representation of the space inter-membranes filled by the solution excluding the transversal section of the filaments (Figure 3d). For high rejection membranes, it would not be necessary to define a domain for the membranes as their effect on the fluid domain can be implemented in the lower and upper boundaries.

It is important to point out that the average flow and the average concentrations along the z-coordinate present small variations from input to output compared to the gradients of velocity and the concentration inside the domain. Therefore, the domain can be considered as a repetitive pattern in the *z*-coordinate. As a consequence, a length of domain only corresponding to a small number of spacers is needed.

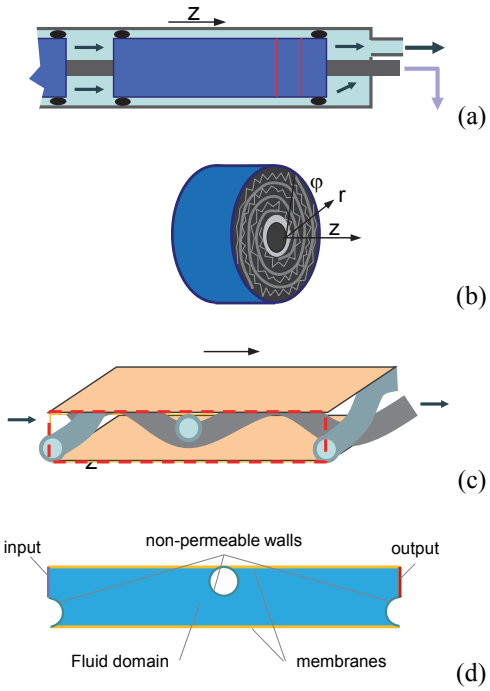

Figure 3. Specification of the domain of study (a-d) and boundary specification (d).

3. Case of study

In the following lines the conditions used as an example to illustrate the application of the simulation are described.

The distance between the upper and lower membranes corresponded to a channel height of h= 1 mm and a length corresponding to twice the distance between two consecutive spacers (L=6 mm). The diameter of the spacer filament was d = 0.5 mm.

The study was apply for generic low-pressure reverse osmosis membrane. A water permeability coefficient of 2.1 $cm^3 \cdot m^{-2} \cdot s^{-1}$ was used, as a value inside the range of this type of membranes. As reverse osmosis membranes exhibit high ion rejection, for the sake of simplicity, total ion rejection was assumed.

The operating variables were a temperature of 25 ºC and a pressure of 5 bar. The input flow corresponded to an average cross-flow velocity of 0.25 m/s.

Two ionic systems were selected to illustrate scaling either by calcium carbonate or by gypsum (Table 1). Both systems include ions belonging to a non-precipitant salt (NaCl) together with ions of the precipitant salt. The ions from NaCl were included to have an ionic strength comparable to that of a real feed solution. Table 1 shows the compositions for concentrate solutions that were chosen to be near to scaling conditions at a pH of 6.7.

Table 1: Composition of the solutions studied

System	Ions	Concentration ($mol \cdot m^{-3}$)
I) Calcite scaling prone system	Na^+	20
	Cl^-	20
	Ca^{2+}	3
	$HCO_3^- + CO_3^{2-}$	3
II) Gypsum scaling prone system	Na^+	20
	Cl^-	20
	Ca^{2+}	6
	SO_4^{2-}	6

4. Modeling equations

The following phenomena are relevant to model the scaling potential during the concentration process:

- Flow of solution inside the channel in the direction from feed to concentrate.
- Water permeation through the membrane driven by the pressure difference existing between feed-concentrate and permeate sides.
- Concentration polarization of ions.
- Salt precipitation, under specific chemical conditions.

4.1 Flow of solution

The flow of solution in the membrane channel was defined by the Navier-Stokes equations simplified for the case of an incompressible fluid. A complete set of the equations can be seen in [3].

4.1 Mass transfer in the solution

The Nernst-Planck Equations including the convective transport imposed by the velocity field are appropriate to model the ionic transport in the solution. See [4] for a complete description of these equations.

4.2 Membrane modeling

According to the solution-diffusion model, the driving-force for the volumetric flux is the difference in effective pressure (applied pressure minus osmotic pressure) between both membrane sides:

$$J_v = A_w \cdot (\Delta P - \Delta \Pi) \quad (1)$$

The osmotic pressure for an ionic solution at moderate concentrations is well described by the Van't Hoff's equation that depends on the total molar concentration of ions and the absolute temperature:

$$\Pi = C \cdot R \cdot T \quad (2)$$

By assuming total rejection, the osmotic pressure in the permeate stream is zero. If total rejection were not assumed, the flux of ions through the membrane could be calculated implementing a more complex membrane model, as the authors did in previous works [5, 6].

4.3 Langelier Saturation Index (LSI)

The scaling potential of calcium carbonate can be estimated by the Langelier Saturation Index, which is calculated in the concentrate stream as follows:

$$LSI = pH - pH_s \quad (3)$$

where pH is the value measured or estimated for the concentrate stream and pH_s is the pH at which the concentrate stream is saturated with $CaCO_3$. The latter value is calculated using the following equation:

$$pH_s = pCa + pALK + IF \quad (4)$$

The term pCa is obtained from the concentration of calcium ion in the concentrate

(Ca) in mg/L (expressed as equivalent calcium carbonate):

$$pCa = 5 - \log(Ca) \quad (5)$$

In the same way, the alkalinity value in the concentrate (ALK) is used to evaluate the term $pALK$ as:

$$pALK = 4.7 - \log(ALK) \quad (6)$$

where ALK is the sum of carbonate and bicarbonate expressed as mg/L of equivalent calcium carbonate. The carbonate ion is at low concentration compared to the bicarbonate ion, and it can be related with the bicarbonate concentration and the pH.

The incrustation factor IF in Eq. 4 can be obtained from a chart [7] as a function of the total dissolved solids in the concentrate and the solution temperature.

4.4 Gypsum saturation percentage

The calcium sulfate scaling potential is calculated from the concentration of the calcium and the sulfate ions in the concentrate stream:

$$K_{sp} = [Ca^{2+}] \cdot [SO_4^{2-}] \quad (7)$$

The solubility product (K_{sp}) is determined as a function of the ionic strength of the concentrate stream at the operation temperature. The percentage of gypsum saturation is defined as:

$$GSat(\%) = \frac{K_{sp}}{[Ca^{2+}] \cdot [SO_4^{2-}]} \times 100 \quad (8)$$

5. Use of COMSOL Multiphysics

5.1 Geometry

The 2D geometry of the domain shown in Figure 2d was built by difference between a rectangle and circles representing the cross section of the filaments.

5.2 Domain and global definitions

The COMSOL Flow mode was used to model the hydrodynamics conditions of the membrane system. Considering that sodium and chloride ions were the major ions in solution, the density and viscosity of the solution were those corresponding to a NaCl solution of the same total concentration. The following correlations were used to take into account the dependence of the properties on the mass fraction of the salt, m_A [8]:

$$\rho = 997.1 + 694 \cdot m_A \quad (9)$$

$$\mu = 0.89 \times 10^{-3} \cdot (1 + 1.63 \cdot m_A) \quad (10)$$

The Nernst-Planck Equations mode was used to model the ionic transport in water. The velocity field calculated by the flow model was used for the convective terms. In both composition cases, sodium was selected to be calculated from the electroneutrality condition.

The osmotic pressure (Eq. 2) was defined as an analytical function of the concentration. The LSI was defined as an analytical function built by combining Eq. 3 to 6 as a function of pH, calcium and bicarbonate concentrations and the incrustation factor IF. The IF was an interpolation function defined from tabulated values. Other necessary data for the transport model were the ion diffusivities at the operating temperature (Table 2).

Table 2: Ion diffusivities at 25 ºC [9]

Ion	Diffusivity m^2/s
Na^+	1.33E-09
Cl^-	2.03E-09
Ca^{2+}	0.718E-09
HCO_3^-	1.183E-09
CO_3^{2-}	0.95E-09
SO_4^{2-}	1.060E-09

5.3 Boundary conditions

The membrane model was included in the boundary conditions for flow and mass transfer in the membrane boundaries.

The boundary conditions for the flow physics were defined as follows:

First, it was taken into account that the domain is a repetitive pattern, and that the permeate flux was of a magnitude much smaller than the velocity in the channel. Then, a periodic boundary condition between the input flow and the output flow was set by varying the pressure drop from inlet to outlet until the desired inlet flow was obtained. It was also necessary to specify a pressure condition in an arbitrary corner of the output boundary because the operating pressure cannot be arbitrarily fixed as this variable affects the membrane flux. At the boundaries representing the membranes, the flux was calculated using Ec. 1 and the analytical function for osmotic pressure. Regarding to the spacers a wall condition was used.

The boundary conditions for the Nernst-Planck mode were the following:

At the membrane and spacer surfaces a No-flux condition was imposed. Input was defined using pre-specified bulk concentrations and the output was a convective output.

5.4 Mesh

The mesh used for the bulk of the fluid was a free-triangular mesh calibrated for a fluid dynamics problem. A predefined mesh size "finer" was chosen as this size was small enough to assure cell Reynolds number under 3 in almost the whole domain for all cases. At the membrane and spacers walls, a boundary layer was used with stretching factor of 1.2 and thickness adjustment factor of 5.

5.5 Solving procedure

To assure convergence, the solving procedure was structured in the following steps:

1) calculation of the hydrodynamics independently from concentration,
2) calculation of the ionic transport without hydrodynamics,
3) calculation with a segregated solver of both modes together.

The direct solver used was PARDISO.

The parametric sweep followed the same sequence.

4. Results

The results obtained in the calcium carbonate scaling study and those of the gypsum study are shown below. In the case of the calcium carbonate solution a parametric study for cross-flow velocity is also illustrated.

4.1 Calcium carbonate scaling

The conditions of the case of study were chosen to have LSI values in the bulk solution slightly lower than zero. Fig. 4 shows the LSI mapping and the flow streamlines in the zone near to a spacer. It can be seen that the LSI values are greater than zero in the membrane areas near to the base of the spacer. These areas have possible calcium carbonate scaling as a consequence of their low cross-flow velocity.

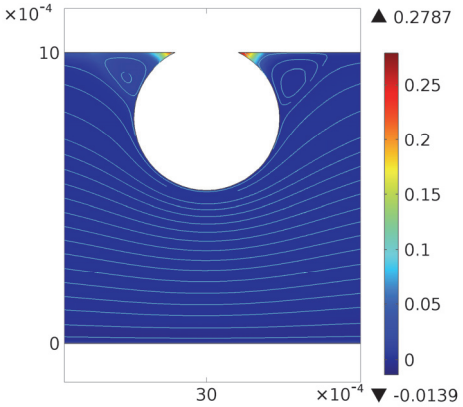

Figure 4. Flow streamlines and LSI mapping.

Fig. 5 shows clearly that the solution over the whole membrane area has LSI values slightly over zero. This implies calcium carbonate scaling in the long term. This situation can be changed taking proper measures. For example, the concentration obtained could be used to calculate the acidification need to achieved safer values of LSI.

Besides concentration and pH, the LSI can be affected by hydrodynamics conditions. For example, Fig. 6 shows a parametric study of the effect of the cross-flow velocity, defined as flow per channel section excluding spacers, on the fraction of area subjected to potential scaling. The figure was obtained by using the pressure drop between inlet and outlet as a parameter ranging from 3000 to 50000 Pa. Couplings

variables were defined for the average value of the LSI on the lower membrane and the integral of the velocity in the inlet. The figure shows the strong reduction of the fraction of the membrane area under scaling conditions from 100% to less than 10%. This reduction is a consequence of the decrease of the concentration polarization effect.

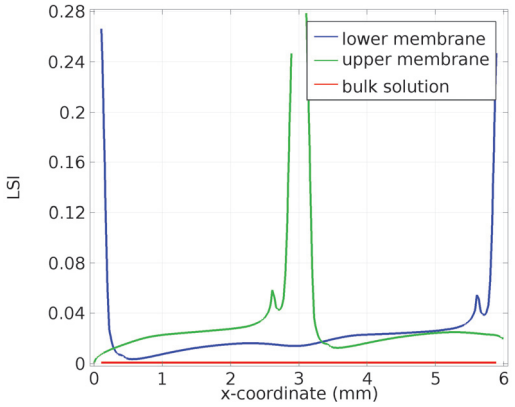

Figure 5. Langelier Saturation Index calculated using bulk concentrations at both membrane sides for the conditions used in this study.

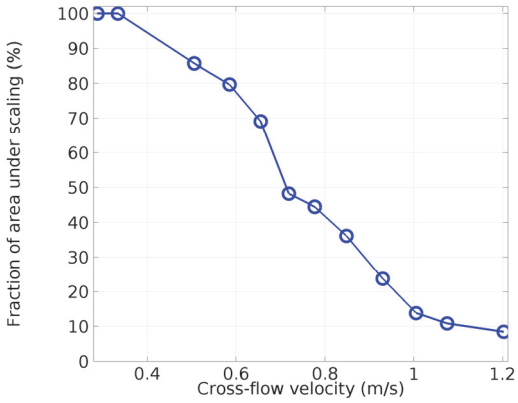

Figure 6. Fraction of membrane area under scaling condition of LSI>0 at different cross-flow velocities.

4.1 Gypsum scaling

Seemingly, Fig. 7 shows a case of gypsum scaling calculation on the membrane surfaces. In this case, the calculation for this case II using ion bulk concentrations shown in Table 2 yielded a saturation percentage of 73.5% what indicates that scaling is apparently not produced. However, the scaling calculation with the ionic concentration values achieved owing to the concentration polarization phenomenon indicated a similar situation to that obtained for the calcium carbonate system. Again, it can be seen that the scaling parameter is higher in the areas near to the spacers, and that even gypsum precipitation occurs at same points (saturation > 100%).

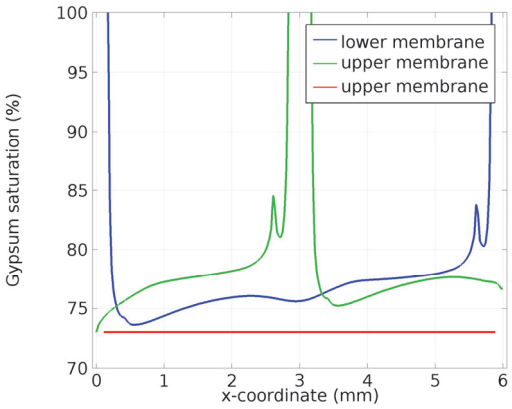

Figure 7. Gypsum saturation calculated using bulk concentrations at both membrane sides for the conditions used in this study.

7. Conclusions

The results of this study showed the convenience of modeling the concentration polarization phenomenon taking into account the internal geometry of the membrane channel to correctly estimate the scaling potential. To demonstrate this point, we have shown some situations with localized salt precipitates for which scaling was not expected according to bulk concentration.

The information provided by the developed model can be useful to set suitable chemical and operating conditions in the concentrate to assure that scaling is not produced at any point of the membrane.

8. References

1. J. Schwinge et al, Simulation of the flow around spacer filaments between channel walls: Mass-transfer enhancement, *Ind. Eng. Chem. Res*., **41** 4879–4888 (2002).
2. A.L. Ahmad et al., Integrated CFD simulation of concentration polarization in narrow

membrane channel, *Computers and Chemical Engineering*, **29**, 2087–2095 (2005)
3. COMSOL Inc., CFD module. User's guide, 27-143 (2012)
4. COMSOL Inc, Chemical Reaction Engineering Module. User's guide, 142-156 (2012)
5. J.M. Gozálvez-Zafrilla, A. Santafé-Moros, Implementation of the DSPM model using a commercial finite element system, *Desalination*, **250**, 840–844 (2010)
6. J.M. Gozálvez-Zafrilla, A. Santafé-Moros, Nanofiltration Modeling Based on the Extended Nernst-Planck Equation under Different Physical Modes, Comsol Conference Hanover (2008)
7. Dow Liquid Separations, Form no. 609-00071-0705, Technical Manual (Electronic document)
8. Geraldes et al., Flow and mass transfer modelling of nanofiltration, *Journal of Membrane Science*, **191**, 109-128 (2001)
9. Y-H. Li, Diffusion of ions in seawater and in deep seawater sediments, *Geochimica et Cosmochimica Acta*, **38**, 703-714 (1974)

9. Acknowledgements

The Spanish Ministry for Science and Innovation is kindly acknowledged (Project OPTIMEM, CTM2010-20248).

10. Appendix

Table 1: List of symbols

Symbol	Definition and SI Units
ALK	Total alkalinity, $mol \cdot m^{-3}$
A_w	Water permeability, $m^3 \cdot m^{-2} \cdot Pa^{-1}$
Ca	Calcium ion in the concentrate, mg of equivalent calcium carbonate per liter
C_f	Ion concentration in the bulk solution, $mol \cdot m^{-3}$
C'_f	Ion concentration in the solution at the membrane wall, $mol \cdot m^{-3}$
$GSat$	Gypsum saturation index, %
IF	Incrustation factor
J_v	Volumetric flux, $m^3 \cdot m^{-2} \cdot s^{-1}$
K_{sp}	Gypsum solubility product, $mol^2 \cdot m^{-6}$
LSI	Langelier Saturation index
m_A	Mass fraction of salt
pH_s	pH at calcium carbonate saturation
R	Gas perfect constant, $8.314\ J \cdot mol^{-1} \cdot K^{-1}$
T	Absolute temperature, K
ΔP	Applied pressure difference between both membrane sides, Pa
$\Delta \Pi$	Osmotic pressure difference between both membrane sides, Pa
ρ	Density, $kg \cdot m^{-3}$
μ	Viscosity, $Pa \cdot s$